Energy Conversion and Management 354 (2026) 121242

Contents lists available at ScienceDirect

Energy Conversion and Management

journal homepage: www.elsevier.com/locate/enconman

Research paper

Assessing the replicability of optimal control for GSHP integrated with PV and battery storage in different European renovation scenarios

Sarah Noye [a], Laura Carnieletto [b,*], Michele De Carli [c]

[a] TECNALIA, Basque Research and Technology Alliance (BRTA), Mikeletegi Pasealekua 2, Donostia-San Sebastián, 20009, Spain
[b] Department of Environmental Sciences, Informatics and Statistics, Ca' Foscari University of Venice, Via Torino, 155, Mestre, 30172, Italy
[c] Department of Industrial Engineering, University of Padova, via Venezia 1, Padova, 35131, Italy

ARTICLE INFO

Keywords:
Ground source heat pump
Photovoltaic
Battery
Control
Genetic algorithm
Time of use energy tariff

ABSTRACT

Residential buildings that combine a ground source heat pump (GSHP), photovoltaic (PV) panels and a battery can increase self sufficiency and provide services to the grid. In Europe, the variability of solar production together with time of use tariffs makes the operational cost of such installations highly sensitive to the control strategy.

Current control strategies are either sub-optimal reactive rules that ignore future operation, or sophisticated model-predictive controllers that require an accurate plant model and must be re-tuned for every new building. Consequently, a simple, yet robust, control system that can be directly reused across many cases remains an open problem.

A Genetic Algorithm (GA) is employed to generate a 24-hours schedule. Each chromosome contains 24 numbers $x_t \in [-1, 1]$. The sign defines the action (discharge, idle, charge), the absolute value the fraction of the available power. The GA was applied to a pre-existing database of GSHP yearly energy consumption. For each of the 87 case studies (3 climates×6 retrofit levels×4 PV orientations for different building types) the algorithm minimises the electricity-purchase cost over a 24-h horizon.

Compared with a rule-based baseline, the GA reduces the annual electricity bill by up to 30% and by around 250 €/y. The algorithm performs better in climates with more intermittent solar production. The terraced-house archetype shows the highest relative savings because PV production and demand are balanced. Deeper retrofits increase relative savings while absolute savings drop and larger intra-day price spreads drive higher relative savings, demonstrating the controller exploits price fluctuations.

1. Introduction

1.1. Background

The European Union (EU) target of reaching at least 42.5% of renewable energy by 2030 [1] drives the need for low-carbon heating and cooling solutions. Ground source heat pumps (GSHPs) are attractive low temperature HVAC because they operate on a stable ground temperature, and can be fully powered by electricity [2]. When a GSHP is coupled with photovoltaic (PV) panels and a battery, the building has the potential to meet its heating, cooling and electricity demand with renewable energy [3]. Such coupling has been demonstrated to increase system flexibility and to enable tariff-aware cost reductions and peak shaving in buildings and districts [4] while reducing green house gas emissions [5]. Using proper control strategies, this coupling offers the possibility to increase the consumption of energy that is self-produced through PV, which can be further maximised if operating with a storage battery [6,7]. A well sized system is key to limit initial investments [8], but control strategies can also enable to optimise the operational costs while maximising self-consumption and self-sufficiency [9].

Although many systems still rely on reactive, rule-based control because it is simple to deploy at scale, such strategies struggle with complex grid interactions and dynamic price signals [10]. Advances in forecasting are improving the accuracy of energy production and demand predictions [11], handling the high uncertainty linked with occupants' behaviour. This trend enables the rise of predictive control, which is particularly interesting for capitalising on price signals designed to ensure the stability of the electrical grid. To achieve broad impact, however, control algorithms must be both replicable (i.e., transferable across diverse systems without bespoke redesign) and applicable at scale (i.e., computationally and operationally viable).

* Corresponding author.
E-mail address: laura.carnieletto@unive.it (L. Carnieletto).

https://doi.org/10.1016/j.enconman.2026.121242
Received 20 December 2025; Received in revised form 2 February 2026; Accepted 14 February 2026
Available online 23 February 2026

Nomenclature

Abbreviations

AB	Apartment Block
BL	Baseline Control Algorithm
CDD	Cooling Degree Days
COP	Coefficient Of Performance
DHW	Domestic Hot Water
EER	Energy Efficiency Ratio
FC	Fan coil
GA	Genetic Algorithm
HVAC	Heating, Ventilation, and Air Conditioning
GSHP	Ground Source Heat Pump
HDD	Heating Degree Days
HP	Heat Pump
OB	Office Building
PV	Photovoltaic
RAD	Radiant System
RS	Random Search Algorithm
SoC	State of Charge of the battery
TH	Terraced House
VAT	Value Added Tax [%]

Symbols

Cap_{max}	Useful capacity of the battery [kWh]
Cap_{rated}	Rated capacity of the battery [kWh]
E_t	Energy charged or discharged from the battery at time t [kWh]
L_c	Probe length to satisfy the cooling load [m]
L_h	Probe length to satisfy the heating load [m]
$loss$	Charge and discharge loss of the battery [0-1]
P_L	Electrical load [kWh]
P_{max}	Maximum power to be exchanged with the grid during a time step [kW]
P_{PV}	Electricity produced by the solar panel [kWh]
Q_{demand}	Heating and cooling demand of the building [kWh]
R_{buy}	Cost of electricity purchased from the grid [€/kWh]
r_{elec}	Daily ratio of photovoltaic production to electrical demand [–]
SoC_t	State of charge of the battery at time t [0-1]
SoC_{min}	Minimum allowable state of charge of the battery [0-1]
U	Thermal transmittance [W/(m^2 K)]
x_t	Percentage of charge (positive) and discharge (negative) [−1,1] to apply at time step t
μ	Mean
σ	Standard deviation

When examining the literature, fully integrated GSHP–PV–battery control remains relatively scarce [12,13]. Therefore, the classification presented here also draws on closely related studies on battery scheduling. Within this combined evidence base, approaches to battery schedule optimisation can be organised into three methodological families: (i) Rule-based reactive control, (ii) Deterministic optimisation methods, (iii) Heuristic optimisation methods. This structure enables a systematic discussion of methodological assumptions, typical optimisation objectives, and deployment constraints across related system configurations.

Rule-based reactive control. Priority-based logics, threshold rules, and decision trees are widely used in practice due to simplicity and low commissioning effort. They have been applied, for example, to preheat domestic hot water (DHW) using PV surplus [12], or to orchestrate GSHP operation with PV forecasts [13]. Chakir et al. proposed a diagram flow for a PV–battery system based on performance equations of the system [14]. While easy to deploy, these approaches are limited in handling complex multi-objective trade-offs or variable prices and typically require case-specific tuning, which constrains replicability.

Deterministic optimisation methods. Formulations based on linear programming, mixed-integer programming, and dynamic programming target objectives such as cost minimisation, peak shaving, emissions reduction, battery life, or capacity planning. Examples include linear programming for peak-load management [15], linear programming-based energy management system for electricity bill minimisation [16], and dynamic programming to maximise owner daily profit while mitigating over-voltage problems [17]. Despite strong performance when models are accurate, in their review on optimal energy management for battery energy storage, Yang et al. found that the main limitation of linear programming is the requirement of a well defined mathematical problem, while dynamic programming is computationally intensive [18]. As a result, portability across many buildings and scenarios are often limited.

Heuristic optimisation methods. Fuzzy controllers offer flexibility and are relatively easy to implement and have been demonstrated for PV-battery coupling [19], but they rely on expert-defined membership functions and rules that are highly case-dependent, reducing replicability [9]. Yang et al. [18] identifies heuristic methods as simple to implement, flexible and fast to converge, while Judge et al. highlight meta-heuristic methods and particularly genetic algorithms (GA), as effective for energy management and scheduling under uncertainty [20]. Meta-heuristics algorithms are especially attractive for non-linear, non-convex search spaces. Their main limitation is that they do not guarantee global optimality like deterministic optimisation methods do[21]. For battery scheduling, several nature-inspired meta-heuristics have been studied [22]. In particular, GAs exhibit strong global search capability and broad practical performance [23], with demonstrated relevance for PV–battery scheduling [24,25].

Across these families, common optimisation objectives include: (1) Cost optimisation, (2) Battery capacity optimisation, (3) Battery life optimisation, (4) Emission optimisation [22]. Application scenarios range from PV–battery systems and DHW scheduling [12,13], to PV–battery coordination for peak shaving and cost reduction [14–17]. In the case of system with GSHP, minimising operational cost enables the reduction of the overall cost, which is the main barrier for the wide implementation of such systems and will be the focus of this study.

Despite promising results, practical limitations recur in the literature and hinder wide adoption: (i) *Case-dependent design and modelling.* Many predictive and optimisation methods depend on detailed, site-specific models, constraints, and calibration pipelines. This reliance reduces replicability across different buildings, climates, and retrofit conditions. (ii) *Limited cross-scenario validation.* Smart control approaches are often validated on a single case, making their generalisability and transferability unclear.

1.2. Research gap and contribution

While systems including GSHP, PV and batteries have a positive impact on the grid and while GA shows promises as means to control them, no study has demonstrated a simple, out of the box optimisation

that can be applied unchanged to a wide variety of building archetypes, climates and retrofit levels. Existing investigations are typically limited to a single building or a narrow set of operating conditions, preventing an assessment of the transferability required for real world, large scale roll out necessary to for achieving significant greenhouse gas reduction. This paper aims to bridge this research gap towards large scale replicability.

This paper builds on the evaluation of geothermal and photovoltaic installation performance performed in [8] for different archetype buildings, climates and renovation scenarios. The hourly electricity demand data from typical historic and existing urban buildings in three European climates (warm, mild, and cold) according to the archetypes defined in [8], have been used to build a database of 87 scenarios to evaluate control performance. The study also draws on the conclusions from the review of smart control performed in [9].

This study makes three contributions aimed at replicability and scaling: (i) *A simple, model-free GA formulation with compact, transferable encoding.* The paper introduce a ternary continuous genetic algorithm (GA) in which each chromosome contains 24 genes which sign selects one of three mutually exclusive actions (discharge, idle, charge) and the magnitude defines the fraction of the available power exploited, providing a model free, compact encoding applicable to any GSHP–PV–battery system, facilitating replication without bespoke reformulation; (ii) *A large-scale, cross-scenario evaluation* by benchmarking the GA on a large scale database of 87 scenarios generated in the Horizon 2020 GEO4CIVHIC project. This broad evaluation directly addresses the literature's lack of cross-scenario validation and assesses transferability at scale; (iii) *Actionable insights for challenging cases.* The least favourable scenarios are analysed to identify strategies to mitigate their limitations, paving the way for a large-scale impact on PV self-consumption and green house gas emissions reduction. The proposed method is designed to support the future energy transition by enabling scalable and adaptive solutions for zero energy buildings and energy communities. To do so, the following research questions are considered: (1) How can a GA-algorithm make use of the energy market prices to increase the efficiency of a PV, battery and GSHP combined system? (2) How well does a GA-based control transfer between different use cases? Despite ongoing research in the field, to the best of the authors' knowledge this is the first study that systematically compares the benefits of intelligent control across such a wide range of configurations, climates, and user profiles. This work thus represents a significant step towards the broader adoption of smart energy management solutions, supporting the scalability and replicability of decentralised renewable energy systems in diverse contexts, including future climate scenarios.

The paper is structured presenting the methodology in Section 2, which is divided in two main subsections: a description of the archetypes used as control optimisation case studies, and the optimisation strategy together with the algorithm validation and evaluation methods. Section 3 shows the main results, comparing different climate and retrofit scenarios and investigating the influence of energy prices. Section 4 and Section 5 discusses the main outcomes and summarises the main findings, gathering the main advantages and limitation of a simple GA predictive algorithm for large scale optimisation of photovoltaic panels and storage systems coupled with GSHP.

2. Methodology

2.1. Methodology overview

This study uses as basis the building archetypes defined in [8]. These buildings combined a GSHP system for heating and cooling and a PV system to supply both the electrical demand of the HP and other electricity needs of the building. For this study, a electrical battery is also considered to store the excess PV production and to get energy from the grid when energy prices are low to avoid buying energy from the grid when prices are high.

A control algorithm was developed to optimise the use of the battery, thus to minimise the energy cost, while maximising self-consumption and self-sufficiency to have the heating and cooling provided as much as possible with renewable energy. Fig. 1 illustrates the different elements of the control system and the information flow between them.

Three building typologies have been investigated considering several renovation scenarios and three climates (cold, mild and warm), analysing their influence on the outcome of the optimisation algorithm.

2.2. Definition of the control use cases

2.2.1. Archetypes definition

The research carried out by Carnieletto et al. [8] describes in details the buildings archetypes selected as relevant for GSHP systems in the European urban context considering a typical warm (Athens), mild (Strasbourg) and cold (Helsinki) location (see detail about climate selection in Appendix A.1). A summary will be presented in this paper, focusing on the estimation of electric energy demand and production since they are the main inputs of the control algorithm.

The main representative types of buildings located in urban areas within the European building stock have been distinguished into three main archetypes as illustrated in Fig. 2:

- Terraced House (TH): independent land-to-sky building with one or two floors.
- Apartment Blocks (AB): large buildings divided into apartments.
- Office Buildings (OB): apartment blocks converted to office end use, typically present in European city centres.

The terraced house has been studied considering a typical residential use, while the apartment block has been simulated both for residential and office use. The space heating and cooling energy demand was estimated based on dynamic simulations carried out with the software TRNSYS 17 [27]. Buildings were simulated considering detailed thermal zones with different envelope properties based on the period of construction: if the building was built before 1950, it was defined as historic, otherwise (construction after 1950) it was described as existing building. The main characteristics and the input of the model have been reported in Appendix A.2.

The seasonal values of heating and cooling energy demands as well as the peak load have been determined by 36 dynamic simulations. The results have been validated against the previous project Cheap GSHPs [28] and the TABULA WebTool [29] and a good matching has been obtained. The energy demand profiles and the peak power obtained have been used to size the geothermal probes. More details on these results are presented in [8].

The main focus of this paper will be on the results obtained for terraced houses, because the size of the PV system for this archetype better matches both the load required and the need to find a proper strategy to use or store the energy produced based on the market prices, which showed extreme variability in the last years. When considering apartment blocks and office buildings, the available space is not always sufficient to guarantee sufficient renewable energy production for each user.

2.2.2. Renovation scenarios

The renovation scenarios are the ones used in [8] and are based on applying GSHP systems as retrofit action for existing and historic buildings in urban city centres. The existing system was considered to be a standard boiler coupled with traditional radiators; summer cooling was not included as existing system because their installation has become widespread only in recent years. Due to the wide presence of high temperature terminals and historic buildings listed as protected cultural heritage, the strategies proposed can be used to couple high temperature GSHPs with existing radiators; however, to

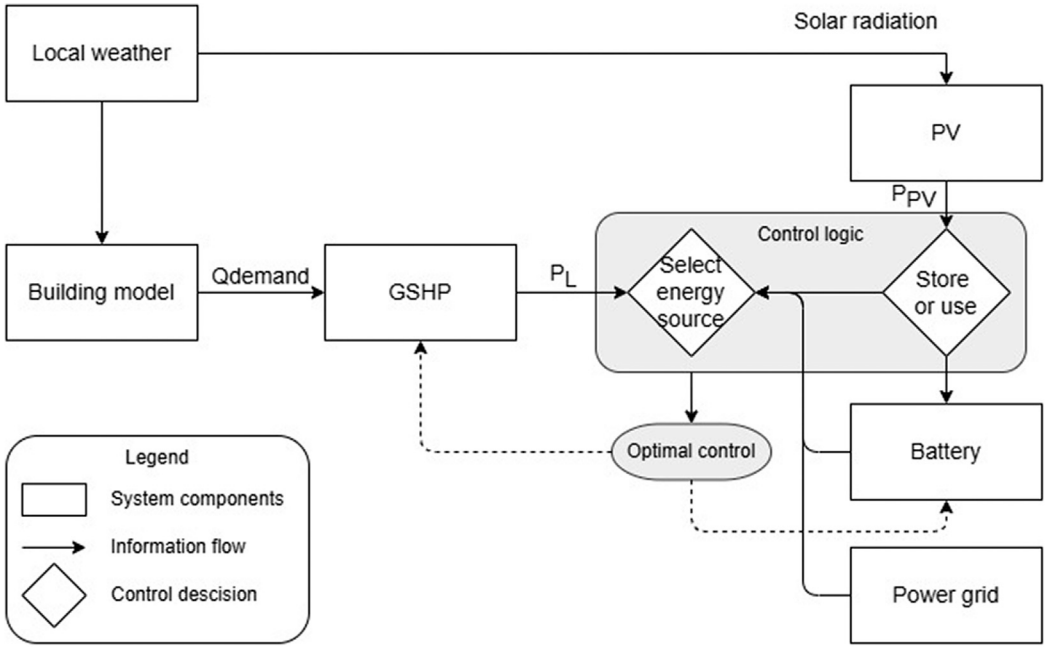

Fig. 1. Optimisation algorithm workflow for multi-renewable energy integration.

Fig. 2. Example of building archetypes for terraced house, apartment block and office building [26].

increase the overall efficiency of the system, replacing gas boilers with GSHP and radiators with mid to low temperature heating emission systems (i.e. fan-coils and radiant systems) is recommended.

To reduce the energy demand, envelope retrofit has been considered including the insulation of opaque walls applying 12 cm of expanded polystyrene on the inner side. In this way, cultural heritage and urban layout can be protected avoiding reduction of pavement area or pedestrian zone, thus increasing user acceptability. A lower insulation has been considered for internal floors, although separating isothermal zones, to accommodate the potential installation of radiant systems that increase ground source heat pump efficiency by operating at lower temperature [30]. Ground floor and roof insulation aim to achieve the minimum required local transmittance for building retrofit. The potential retrofit solutions considered have been represented in Table 1. Different COP and EER have been considered depending on the type of emission systems and the climate: lower values in case of radiators, due to the high operating temperature that has to be achieved, higher for fan coils and radiant systems (see [8] for more detailed information).

- Existing system: standard boiler coupled with traditional radiators.
- Case 0: standard boiler is replaced with GSHP able to supply high temperature emitters (because radiators are maintained).
- Case 1: standard boiler replaced with GSHP; heating and cooling terminal units are changed with fan coils (FC) or with radiant system (RAD)
- Case 2: standard boiler replaced with high-temperature GSHP; radiators are maintained; insulation of the building is improved.
- Case 3: standard boiler is replaced with GSHP; heating and cooling terminal units replaced either with fan coils or radiant system; building insulation is improved.

For the terraced house, all the renovation scenarios have been considered. For the other cases, only the cases 0, 1 with radiant floor and 3 with radiant floor have been investigated being the most representative for the retrofit strategies applied as they summarise the most common action plans for retrofit, i.e., acting on the generation systems first, with the lowest investment costs; moving to the emission systems, which may involve works on the internal structure, arriving to a complete deep retrofit that includes envelope insulation, which is the most effective in terms of energy reduction but at the same time the most expensive in terms of investment costs. Furthermore, terraced houses have a higher PV capacity installed per user compared to apartment blocks, therefore optimisation could give more interesting outcomes. The installation of envelope retrofit reduces transmission heat losses. As a consequence, the energy demand for space heating is greatly reduced for mild and cold climates, thus the required borehole length for heating, the power required for the GSHP and the electric energy required for the operation. Details about the system sizing have been reported in Appendix A.3.

2.2.3. Photovoltaic panels

To estimate the energy produced and consumed, simulations were carried out using the dynamic tool TRNSYS [27], giving as input information location, inclination and orientation of the panels. The electric load of the building was calibrated based on the energy values provided by Eurostat (Eurostat) for each end use and spread on an hourly base according to profiles suggested by [31]. This hourly production and consumption data were used to evaluate the optimised control presented in this paper. Fig. 3 shows the average hourly consumption of the electrical appliances and lighting by season and day of the week.

Table 1
Retrofit strategies investigated [8].

		Existing system	Case 0	Case 1	Case 2	Case 3
Envelope insulation					X	X
HVAC generation	Gas boiler	X				
	GSHP		X	X	X	X
HVAC emitters	Radiator	X	X		X	
	Fan coil/Radiant			X		X

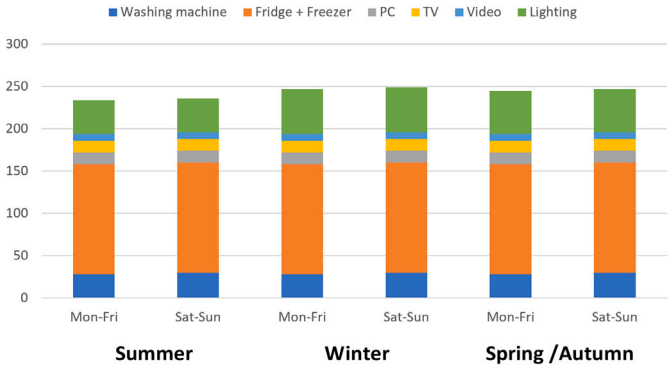

Fig. 3. Average hourly consumption of electrical appliances.

Table 2
Input sizing parameters for PV system modelling.

	Athens		Strasbourg		Helsinki	
	TH	AB/OB	TH	AB/OB	TH	AB/OB
Gross roof area [m^2]	59	416	117	460	121	509
Roof Inclination	0°	0°	30°	30°	40°	40°
Number of panels	18	126	35	140	37	154
Installed Peak Power [kWp]	6.0	41.9	11.9	46.7	12.3	51.7

Starting from the outcomes of the energy simulation, the electric consumption of the heat pump was determined considering the specific COP and EER for each case [8]. Summing the two main loads, the total electric energy was compared with the energy production by the photovoltaic system, which was calculated for four orientations (South, South-West, West, and East) in order to evaluate the efficiency of the system considering the multiple possible orientations of the building in an urban context.

The sizing parameters of the PV system, summarised in Table 2, were defined based on the geometry of the building and the roof characteristics, mostly depending on the considered climate. The available area obtained was further reduced by 5% to consider the space commonly required for technical maintenance. The main difference is on the roof inclination: Athens hosts buildings with horizontal roofs, therefore the space available to install panels inclined by 30° (considered as average optimal inclination) is necessarily limited to avoid mutual shading, hot spots and overheating. As a consequence, the peak power installed is lower compared to Strasbourg and Helsinki. Polycrystalline PV modules typically available on the market were selected. Both for the modules and the inverter technical data have been used as reference for the main inputs.

2.2.4. Battery

A battery system has been introduced in this study to address the intermittence of solar energy production. A Lithium Iron Phosphate ($LiFePO_4$) battery is assumed as it is a common choice for residential storage due to safety considerations and long cycle life. Consistent with commercial $LiFePO_4$ used in residential buildings, 10.53 kWh nominal capacity and 95% useable capacity were assumed, which correspond to 10 kWh useable capacity. The maximum power of the battery, which is the maximum energy that can be charged or discharged from the battery in one hour, is considered to be 5 kW. In line with [32], the efficiency was selected to be 98%.

The model of the battery used for the optimisation considers 4 elements: the capacity of the battery Cap_{max} (10 kWh), the minimum State of Charge (SoC) (0.05), the maximum power P_{max} (5 kW) and the charge and discharge losses (2%). The values used in the study are in parenthesis.

To simplify the implementation, the useable capacity is used as Cap_{max}. The final SoC can then be calculated as follow to take into account the depth of discharge of the battery:

$$SoC_t = (E_t + SoC_{Min} * Cap_{rated})/Cap_{rated} \quad (1)$$

where Cap_{rated} is the rated capacity of the battery and E_t is the energy charged or discharged to and from the battery.

2.2.5. Energy grid and electricity prices

To shorten the return of the investment of the battery, it is interesting to work with a time-of-use tariff, which enables to take advantage of the price signals linked with the relation between production availability and consumption demand. The real time energy prices are extracted via web services from the Entose transparency platform[1], the central collection platform for electricity generation, transportation, and consumption data for the pan-European energy market. The version cleaned by Ember Climate was used[2]. The energy prices from the spot market used belong to the year 2022, and do not include taxes, levies, network charges, subsidies, and supplier's profits. All these parameters can vary significantly between energy providers and country or by regions. The only correction that was made was to add VAT. For electrical energy, in 2022, the VAT was of 20% in France, 6% in Greece, and 24% in Finland.

Fig. 4 shows the energy prices for 2022 for the three considered countries. The yearly variation follow a similar pattern for the three countries. Before and after VAT is applied, Finland has lower energy tariffs than Greece and France. Before tax, France and Greece have similar energy prices, but the VAT being lower in Greece, France has the highest costs in this study.

2.3. Operational optimisation

2.3.1. Problem definition

The objective was to develop a control strategy that optimise the operation of the battery to reduce operation cost and shorten payback time, while achieving high self-consumption and self-sufficiency. The information available for the decision making is the prediction of solar production and energy demand, the current state of charge of the battery and the energy tariffs for the next 24 h.

The object of the optimisation answers the two following questions:

- **When should the energy of the battery be used to power the HP?** To maximise the economic benefit, the energy stored in the battery should be kept for period of high electricity price to maximise the avoided cost per unit of energy supplied.

[1] https://transparency.entsoe.eu
[2] https://ember-climate.org/data-catalogue/european-wholesale-electricity-price-data/

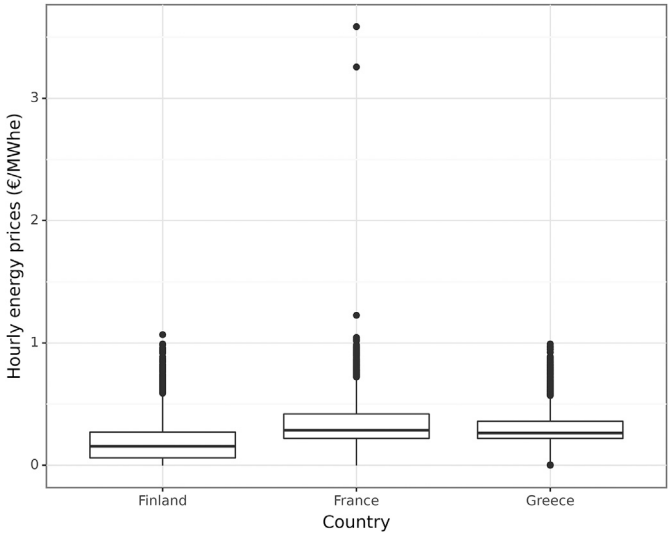

Fig. 4. Hourly energy prices with VAT in the three case study countries.

- **When should energy from the grid be stored in the battery?** If there will be demand to cover at high energy prices, it can be interesting to load the battery at low energy prices.

Since losses are involved both in charging and discharging the battery, the answers to these questions are non trivial.

2.3.2. Control rules

Before the optimisation is performed, the developed control strategy implements the following rules:

1. PV energy (P_{PV}) is used directly by the HP when available. The residual energy to be provided by the grid is the difference between the electrical demand of the HP and other electric systems (P_L) and the PV production when it is positive and is expressed as $max(0, P_L - P_{PV})$.
2. When there is PV energy left, all the energy that fits is stored in the battery.

These enables to make sure that the self consumption is maximised.

2.3.3. Optimisation problem formulation

To solve the optimisation problem, the solution space is modelled in the following way: each individual is defined as a vector of 24 values, each corresponding to the action to be performed in one of the next 24 h.

$$\{x_t\}_{t\in[1,24]} \; where \; x_t \in [-1, 1] \tag{2}$$

The hourly values of the individuals represent three states:

- $-1 \leq x_t < 0$: discharge the battery to cover the electrical demand
- $x_t = 0$: do nothing
- $0 < x_t \leq 1$: charge the battery from the grid

The absolute value $|x_t|$ represents the amount of energy, as a percentage of the available capacity to be charged into or discharged from the battery at time t. It is constrained by the current state of charge (SoC_t) and the maximum allowable power exchange in the micro grid (P_{max}).

The maximum available energy for charging is the minimum of the storage capacity left in the battery ($Cap_{max} \cdot (1 - SoC_t)$ where Cap_{max} is the maximum capacity of the battery) and the maximum power P_{max}:

$$min(Cap_{max} \cdot (1 - SoC_t), P_{max}) \tag{3}$$

Similarly, the maximum available energy for discharging is the minimum between the energy stored in the battery ($SoC_t \cdot Cap_{max}$) and the maximum discharge power (P_{max}):

$$min(SoC_t \cdot Cap_{max}, P_{max}) \tag{4}$$

Note that, if PV energy is used to charge the battery, the exchange power used by the PV is previously removed from P_{max}.

To evaluate the fitness of potential solutions, the objective function is defined as the total cost of electricity bought from the grid over the 24 h window. The optimisation algorithm aims to minimise this function.

The cost for each time step (c_t) depends on the cost of hourly electricity price R_{buy}, the residual HP electrical demand not met by solar PV ($max(0, P_L - P_{PV})$) and the control decision. In the case where the battery is discharged ($x_t > 0$), the energy discharged from the battery, which is the percentage x_t of maximum available energy (Eq. (4)) discounting the discharge losses, is removed from the residual energy to calculate the energy imported from the grid. Because selling energy to the grid is not consider, only positive results are considered. Similarly in the case where the battery is charged ($x_t > 0$), the energy imported from the grid is the percentage x_t of the maximum available energy for charging (Eq. (3)) adding the charging loss. In the case where nothing is done with the battery ($x_t = 0$), the cost is the residual HP demand multiplied by the electricity cost.

The cost as time t is thus calculated as:

$$c_t = \begin{cases} x_t < 0 & R_{buy}{*}max[0, max(0, P_L - P_{PV}) \\ & -(1 - loss){*}min(SoC_t{*}Cap_{max}, P_{max}){*}|x_t|] \\ x_t = 0 & R_{buy}{*}max(0, P_L - P_{PV}) \\ x_t > 0 & R_{buy}{*}[(1 + loss){*}min(Cap_{max}{*}(1 - SoC), P_{max}){*}|x_t| \\ & +max(0, P_L - P_{PV})] \end{cases} \tag{5}$$

The cost of an individual is the sum of hourly costs over the 24 h optimisation horizon ($\sum_{t=1}^{24} c_t$).

2.3.4. Control algorithms

To evaluate the proposed optimisation approach across the diverse case studies considered, three control algorithms were selected to provide a clear comparison framework. The rule-based baseline represents the business-as-usual control strategy commonly implemented in practice, allowing the optimisation benefits to be quantified. Random search is included as a simple meta-heuristic that illustrates the effect of uninformed exploration of the solution space. Finally, a genetic algorithm is used as a lightweight, easily implementable optimisation method that has demonstrated robust performance in similar problem settings.

Baseline control algorithm (BL)

To compare the performance of the optimisation algorithm, a simple reactive rule-based control algorithm was used as baseline.This baseline corresponds to the business-as-usual operation commonly implemented in practice. In this strategy, the demand is covered in priority by the solar panels, then the battery and finally the grid. When a solar energy surplus is available, it is stored in the battery provided its state of charge permits it. In the baseline strategy, the battery is never charged from the grid. It corresponds to an individual where the 24 values are -1 ($\{-1\}_{i\in[1,24]}$).

Random Search (RS)

Random search is included as a simple meta-heuristic benchmark to illustrate the effect of uninformed exploration of the solution space. It consists in sampling the solution space of n individuals successively and at each step compares the current best solution to the new solution and keeps the best one. Although simplistic, random search can occasionally find competitive solutions in large combinatorial spaces and serves as a useful reference for assessing the added value of more structured optimisation approaches. The number of iteration is selected to be the

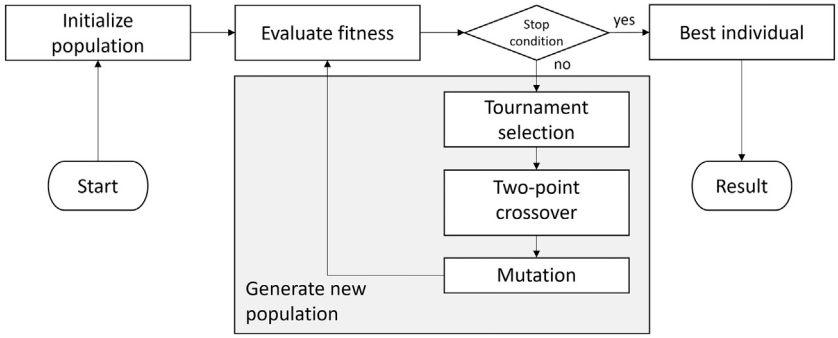

Fig. 5. Genetic algorithm schema Adapted from [9].

population size of the GA times the number of iteration to compare a similar number of individuals.

Genetic Algorithm (GA)

The genetic algorithm serves as the main optimisation method due to its simple formulation, ease of implementation, and suitability for problems involving discrete decision variables. Genetic algorithms iteratively evolve a population of candidate solutions through selection, crossover, and mutation, enabling an efficient exploration of the search space without requiring gradient information or problem-specific adaptations. The GA is not introduced to outperform all possible alternative meta-heuristics, but rather to demonstrate how a lightweight evolutionary approach can robustly improve upon the baseline control strategy across the different scenarios considered in the study.

Similarly to [24,25], this paper uses a standard GA implementation. Fig. 5 illustrate the different steps of the algorithm. First the population is initialised, by generating n individuals of 24 values between $[-1, 1]$. To ensure a balanced distribution between the 3 control states (charge, idle, and discharge) a two steps probabilistic mechanism is used (Eq. (6)). First, a discrete uniform distribution is applied to select between the charge, discharge and idle states. Then, for charge and discharge, a continuous uniform distribution is used to select the percentage of charge/discharge to be performed.

$$x_t = \begin{cases} p_{discreate\_uniform}(-1,0,1) = -1 & p_{continuous\_uniform}([-1,0[) \\ p_{discreate\_uniform}(-1,0,1) = 0 & 0 \\ p_{discreate\_uniform}(-1,0,1) = 1 & p_{continuous\_uniform}(]0,1]) \end{cases} \quad (6)$$

New individuals are generated from the current population by two mechanisms: crossover and mutation. Crossover and mutation are applied to individual or individual pairs if a random number is superior to a defined threshold. The crossover method used was a classic two point mutation where two points are selected randomly and the sequence between those point is exchanged between two randomly selected individuals to create two children individuals.

Similarly to the population generation, a custom mutation methods was implemented to balance the probability to pass from one state to the next. The function first decide whether the stat is being changed and then the value is adjusted by a number following a Gaussian distribution with mean $\mu = 0$ and standard deviation $\sigma = 0.05$.

The fitness of the population is evaluated using Eq. (5). The individuals kept for the next generation are selected with a traditional tournament method, which consists in selecting the best individual among a set of randomly select group of individual of size *trounsize* p times, where p is the size of the population. The process is then repeated for a fixed number of generations.

Based on commonly used settings in genetic algorithms, a crossover probability of 0.5 and a mutation probability of 0.2 were used. The population size was set to 300, with a tournament size of 3, and the algorithm was run for 20 generations, as higher numbers were not improving significantly the results.

2.3.5. Meta-heuristic algorithm validation

Because of the high number of cases considered, a reduced number of test cases were selected for initial validation of the control algorithm. Strasbourg was selected as it represents the mild climate. Regarding the building typology, the existing terraced house was selected as main focus of the study, since the optimisation would have the highest impact. Regarding the retrofitting cases, the selected cases are the cases with only GSHP installation (*Case 0*), the radiant floor (*Case 1*) and the radiant and envelop solution (*Case 3*). Finally, the south west orientation has been considered. This is the most favourable orientation tested after the south orientation in terms of solar production. It has been preferred to the full south orientation because a perfect south orientation is least likely to occur in Europe. Indeed existing retrofit building are not likely to have this orientation and for new building, where orientation is more and more considered, south facing buildings tend to be discarded to avoid overheating from summer solar gains.

To analyse the behaviours of the algorithm, a subset of 10 days was selected according to the daily ratio of photovoltaic production to electrical demand. The ratio is defined as:

$$r_{elec} = \frac{\sum_{n=0}^{23} P_{PV}}{\sum_{n=0}^{23} P_L} \quad (7)$$

The sums are taken over a 24 h period. This ratio captures the relative availability of solar energy compared to demand on a given day, allowing for a diverse selection of scenarios. Values of r_{elec} smaller than 1 correspond to days where the consumption is bigger than the PV production, while values bigger than 1 means that the production is bigger than the consumption. The days were then sorted according to the indicator and 10 equally spaced days were selected for the algorithm validation. The selected days can be found in Table 3.

When performing optimisation for independent days, the initial state of charge (SoC) of the battery is considered to be 20%. This will not account for the influence of the final SoC of the day before, but at this stage, the main interest is to validate the implementation of the GA. The baseline, the random search and the GA control algorithms are compared according to daily cost, and execution time.

2.3.6. Scenario comparison

After validation of the GA algorithm, 87 scenarios were considered to evaluate the impact of the optimised control over a year. The 87 scenarios are divided as follows:

- 72 scenarios based on the existing terraced house case for the 3 climates, the 6 renovation scenarios and the 4 panel orientations;
- 15 scenarios using the three base renovation scenarios with a panel orientation of 45º: 3 scenarios based on the historic terraced house case, 3 scenarios for the existing apartment block, and 3 scenarios for the existing office building, 6 scenarios for the existing terraced house with the Strasbourg climate, but the Athens and Helsinki energy prices. The three base scenarios are the ones selected in Section 2.3.5.

Table 3
Representative days selected for analysis.

Case 0				Case 1 Rad				Case 3 Rad			
Date	Consumption	Panel	r_{elec}	Date	Consumption	Panel	r_{elec}	Date	Consumption	Panel	r_{elec}
07/01/2022	61.59	3.37	0.05	07/01/2022	41.36	3.37	0.08	07/01/2022	24.00	3.37	0.14
12/12/2022	54.50	8.45	0.16	17/12/2022	29.49	6.64	0.23	17/12/2022	18.07	6.64	0.37
14/11/2022	33.89	10.35	0.31	13/02/2022	34.68	15.13	0.44	03/11/2022	15.15	10.87	0.72
08/12/2022	42.61	29.33	0.69	08/11/2022	20.56	18.78	0.91	17/01/2022	18.63	24.76	1.33
14/04/2022	15.61	27.98	1.79	22/03/2022	20.60	39.14	1.90	16/03/2022	12.26	27.07	2.21
18/06/2022	20.10	53.14	2.64	09/03/2022	17.45	47.63	2.73	18/06/2022	17.74	53.14	3.00
30/07/2022	18.84	64.4	3.42	10/10/2022	12.41	43.86	3.54	15/04/2022	13.18	48.4	3.67
05/05/2022	12.35	54.88	4.44	17/08/2022	21.47	96.24	4.48	16/09/2022	17.36	79.02	4.55
25/09/2022	12.62	63.85	5.06	06/08/2022	21.36	108.69	5.09	09/07/2022	19.48	108.33	5.56
20/04/2022	12.30	100.83	8.20	20/04/2022	12.30	100.83	8.20	20/04/2022	12.10	100.83	8.34

The different scenarios are used to analyse how the control strategy performs when the following parameters are changing: building topology and construction date, climate, level of retrofitting, PV panel orientation, and finally energy prices. The building age and topology are evaluated on the validation scenarios. The climate, the retrofitting level, and the PV panel orientation are analysed on the 72 cases for the existing terraced house scenarios. The base case scenarios used for the initial validation have been run with the energy costs of the other two locations, to understand the influence of the energy prices on the optimisation algorithm.

The performance of the optimisation algorithm under the different scenario is analysed in term of operational cost, as other cost, such as initial investment cost do not affect its performance. The operational costs are evaluated according to yearly absolute savings and relative savings compared to the baseline rule-based control cost. The relative savings are calculated as:

$$Relative\ saving = \frac{Baseline\ cost - Optimised\ cost}{Baseline\ cost} * 100 \quad (8)$$

where the *Baseline cost* is the total annual electricity cost under the rule-based control strategy and *Optimised cost* is the total annual cost under the proposed optimisation method. This metric expresses the percentage reduction in cost achieved by the optimised strategy compared to the baseline.

To limit computation power, it was done in steps of 24-hours.

3. Results

3.1. Optimal control validation

The validation of the GA-based control strategy and subsequent tests were conduced in Windows with 32 GB of RAM and an 11th Gen Intel(R) Core(TM) i7-11850H @ 2.50 GHz processor. The code was implemented in Python 3.9 and the GA algorithm was implemented with the DEAP library 1.4.1 (Distributed Evolutionary Algorithms in Python). The GA-based control algorithm was compared with the baseline rule based algorithm and the random search on the three base cases for the 10 representative days with a population size of 300 individuals and a tournament selection size of 3 over 20 generations.

Both the cost of the best solution and the computation time can be found in Table 4. It can be seen that the time of execution of the baseline is almost negligible (less than 1 ms), which is expected as it relies on direct calculations. The average processing time of the GA is 1.23 s for a 24-hours optimisation, however the GA is able to find solutions that are better than the baseline. There is one exception where the baseline is zero and the GA get struck in a local optimal close to zero. Problems of early convergence of GA are wildly documented in the literature and measures to counterbalance it have been investigated [33]. However, since the convergence problem was only observed when the baseline is zero and the cost function cannot be further optimised, it was selected to run the GA optimisation only when the baseline is bigger than zero rather than increase the complexity of the optimisation algorithm. In practice, this enables to save computational power. In comparison, the RS takes in average 7.66 s and only find a solution better than the baseline in 7 of the 30 days tested and those solution are always less good than the GA. The space explored is of the same order of magnitude than the GA (population size time number of iteration), but the GA is much faster because, unlike RS, it reuses good individuals across generations, while RS re-evaluates every candidate independently. The reduced computational power and the better optimisation results demonstrate the exploration power and the validity of GA algorithms.

Table 4
Results on the optimisation for the 10 representative days of the three base cases scenarios.

Case	Day	Cost (€)			Computation time (s)		
		BL	RS	GA	BL	RS	GA
Case 0	07/01/2022	13.08	12.35	11.93	< 0.001	7.00	1.05
	12/12/2022	24.38	21.68	20.16	< 0.001	6.98	1.08
	14/11/2022	4.87	4.10	3.57	< 0.001	6.94	1.06
	08/12/2022	7.14	7.94	5.71	< 0.001	7.01	1.06
	14/04/2022	0.17	0.81	0.12	< 0.001	7.41	1.29
	18/06/2022	0.00	0.55	0.00	< 0.001	8.11	1.33
	30/07/2022	0.00	0.44	0.00	< 0.001	8.17	1.29
	05/05/2022	0.00	0.38	0.00	< 0.001	8.10	1.33
	25/09/2022	0.00	0.38	0.00	< 0.001	8.17	1.20
	20/04/2022	0.00	0.28	0.00	< 0.001	8.04	1.36
Case 1 Rad	07/01/2022	8.34	7.66	7.26	< 0.001	8.29	1.08
	17/12/2022	6.05	5.69	5.25	< 0.001	7.28	1.09
	13/02/2022	2.78	2.47	2.06	< 0.001	7.88	1.07
	08/11/2022	0.41	1.02	0.29	< 0.001	7.33	1.03
	22/03/2022	0.73	1.27	0.58	< 0.001	7.32	1.05
	09/03/2022	0.99	2.26	0.77	< 0.001	7.19	1.03
	10/10/2022	0.00	0.60	0.00	< 0.001	7.20	1.06
	17/08/2022	0.00	0.55	0.00	< 0.001	7.13	1.03
	06/08/2022	0.00	0.26	0.00	< 0.001	7.17	1.06
	20/04/2022	0.00	0.26	0.00	< 0.001	7.17	1.07
Case 3 Rad	07/01/2022	4.27	3.79	3.40	< 0.001	7.15	1.06
	17/12/2022	2.63	2.70	2.25	< 0.001	7.13	1.07
	03/11/2022	0.21	0.67	0.17	< 0.001	7.23	1.42
	17/01/2022	1.36	2.00	1.10	< 0.001	8.32	1.39
	16/03/2022	0.00	0.67	0.01	< 0.001	8.28	1.47
	18/06/2022	0.00	0.48	0.00	< 0.001	8.41	1.43
	15/04/2022	0.00	0.48	0.00	< 0.001	8.47	1.51
	16/09/2022	0.00	1.29	0.00	< 0.001	8.43	1.50
	09/07/2022	0.00	0.30	0.00	< 0.001	8.31	1.62
	20/04/2022	0.00	0.35	0.00	< 0.001	8.26	1.77

Qualitative results for the GA are presented for three types of days on Figs. 6–8. Each of the figure has 3 charts. The top one shows the PV production (green), the energy demand (red) and how the demand is satisfy at each hour of the day (solar energy — green, battery discharge — blue, buying energy form the grid — orange). When the energy from the grid goes above the demand line, it means energy has been bought to charge the battery. Note that the unbalanced power ($P_L - (P_{PV} + P_{Bat})$) at each time step corresponds to the vertical difference between the load curve and the combined contribution of the PV generation and

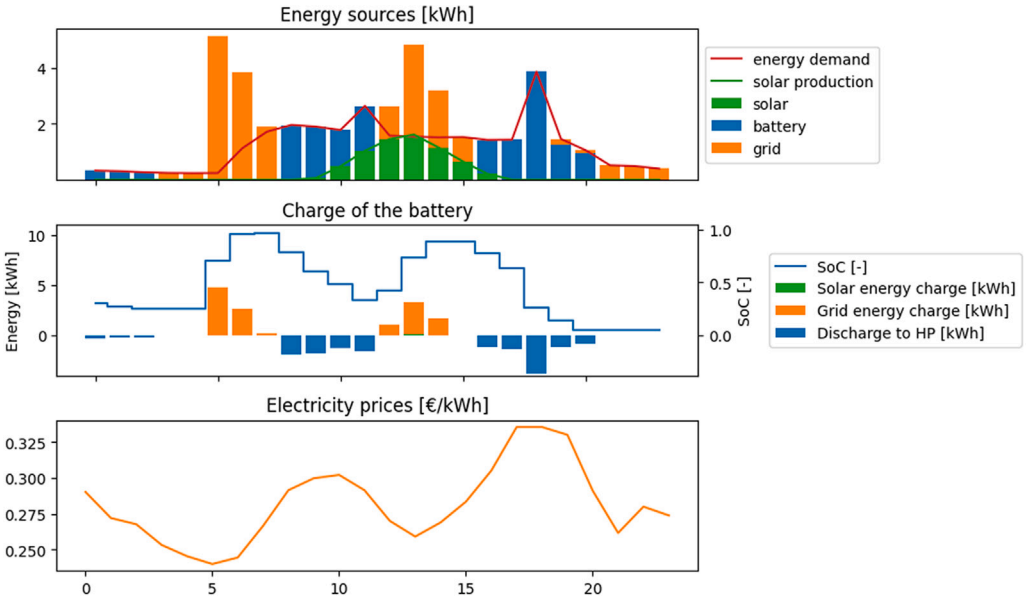

Fig. 6. Example of a day with high demand and low production.

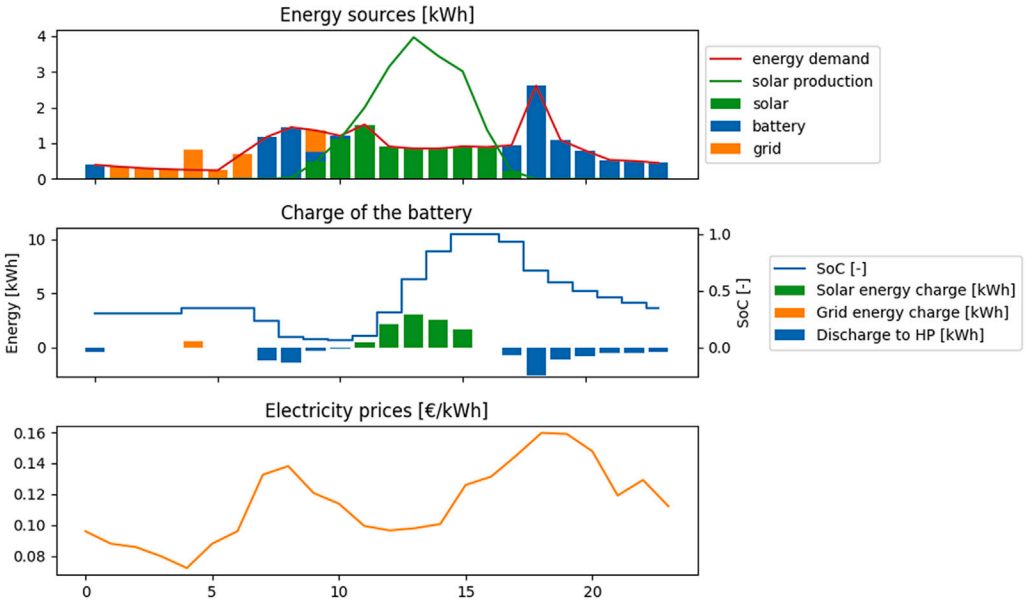

Fig. 7. Example of a day with balanced demand and production.

the battery charge/discharge. The middle chart shows the SoC of the battery, as well as its charge and discharge, while the bottom one shows the electricity prices from the grid.

Fig. 6 shows the results of the GA optimisation for a day where the demand is too high to be covered by the production and where most of the energy of the HP is provided from the grid. It can be seen that the battery is charged when the energy prices are the lowest. Fig. 7 shows a day where there is balance between total demand and total production. It can be seen that the battery is loaded at low energy price time and very little energy is used from the grid the rest of the day. Fig. 8 shows a case where there is more solar production than energy demand. In those cases, the optimal control solution is generally the baseline.

Fig. 9 shows the convergence curve of the GA for those three days. It can be seen that when the optimisation reserve is low (Production > Demand) the GA converges earlier. In the case where the demand is high, the convergence in not fully reached, but test have shown that the improvement was marginal compared to the added computational cost.

3.2. *Influence of the building typology*

Table 5 summarises the cost saving the GA-based control achieves over the rule-based baseline for the references scenarios in different building typologies. It can be seen that the difference is smaller between the different renovation cases for the apartment block and the office building, compared to the terraced house. This is due to the smaller size of the PV system compared to the number of users involved and their overall energy demand in the case of the apartment block and the office building. The relative savings for the terraced house are higher, because there is a better balance between the energy produced and consumed, leading to a higher potential of optimisation. The rest of the study focuses on this case, as it can have a bigger impact if deployed at large scale. However, because the overall energy consumption is

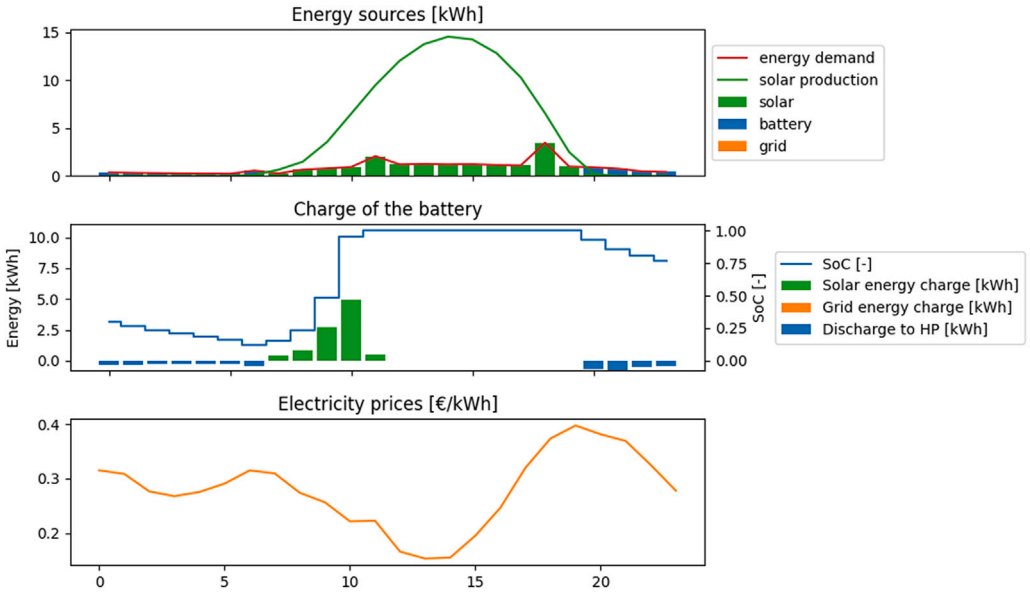

Fig. 8. Example of a day with high production and low demand.

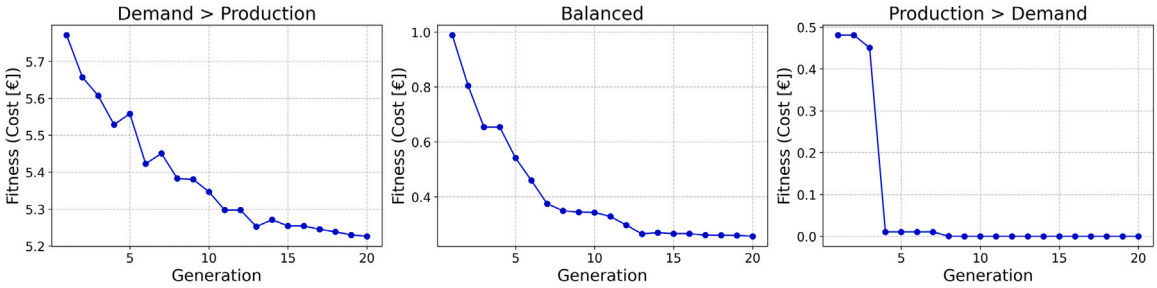

Fig. 9. GA convergence for the three days from Figs. 6–8.

Table 5
Yearly absolute and relative savings achieve by the GA optimisation algorithm for the different typologies.

Type	Case	Absolute Savings (€)	Relative Savings (%)
Apartment block	Case 0	405.22	2.32
	Case 1 Rad	401.02	2.80
	Case 3 Rad	397.07	3.41
Office building	Case 0	473.80	2.46
	Case 1 Rad	473.59	2.46
	Case 3 Rad	472.31	2.45
Terraced house	Case 0	148.91	15.57
	Case 1 Rad	116.01	20.41
	Case 3 Rad	60.11	25.33

Table 6
Yearly absolute and relative savings achieve by the GA optimisation algorithm for the year of construction.

Period	Case	Absolute Savings (€)	Relative Savings (%)
Existing	Case 0	148.91	15.57
	Case 1 Rad	116.01	20.41
	Case 3 Rad	60.11	25.33
Historical	Case 0	170.91	12.55
	Case 1 Rad	138.05	17.42
	Case 3 Rad	68.46	24.89

higher for the apartment block and the office building, the absolute savings are more significant even if they represent a smaller percentage of the energy bill, meaning this type of optimised control can still be interesting in those cases to shorten the payback time of the system.

3.3. Influence of the year of construction

The reference scenarios were compared for two construction periods. Table 6 shows that for existing buildings the relative saving obtained for the control optimisation are higher when the absolute savings are higher for the historical buildings. Since existing buildings have lower losses compared to historical buildings, the optimisation reserve is lower, while the savings achieved have a bigger impact on relative terms. For the same renovation case, the difference is within 3% and 22 € annually. For the deep retrofit case (Case 3 Rad), the difference is smaller as this level of retrofitting bring the energetic performance of both cases closer to one another.

3.4. Influence of the climate

This section summaries how the performance of the GA control algorithm compared to the baseline control is affected by the different climates. Fig. 10 shows that the optimisation algorithm can achieve almost 250 € absolute saving and up to above 30% of energy cost saving compared to the rule-based baseline. The most favourable location for the implementation of the predictive control is Helsinki with absolute saving between 160 €/y and 244 €/y and between 16% and 30% of relative savings. Due to the bigger energy demand and energy bill, there is more room for optimisation, leading to more significant absolute savings.

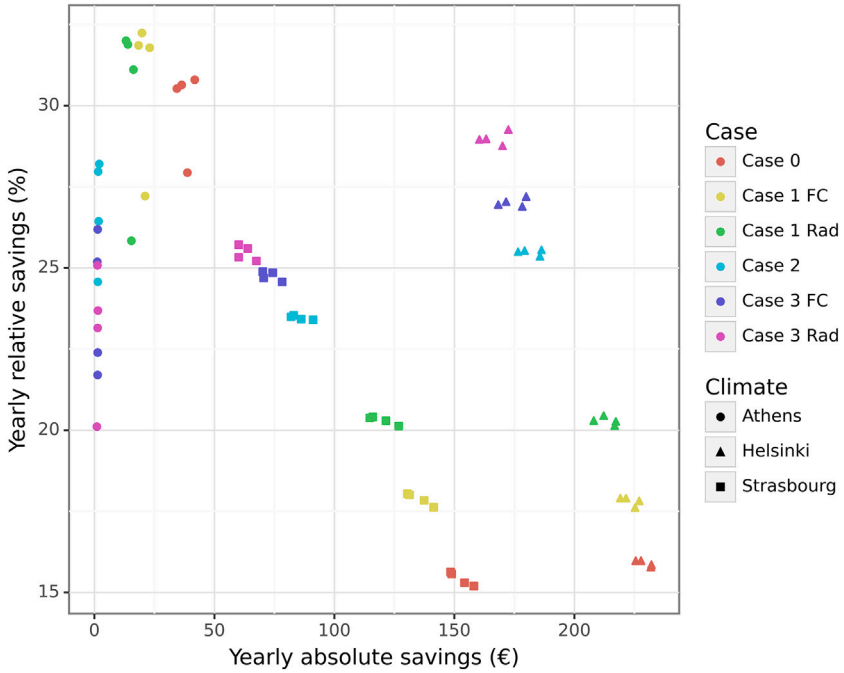

Fig. 10. Yearly relative and absolute savings achieve by the GA optimisation algorithm in different climates and renovation scenarios.

The results are also good for Strasbourg, where the absolute annual savings are between 60 € and 166 € and the relative saving are between 15 and 26%. Those results are less favourable than in Helsinki, because of a lower demand and higher solar production.

In Athens, relative savings are good (20–32%), but the absolute saving are too small to make the implementation of such a control system worth it in the conditions presented in the paper. This is due to a low demand compared to the overall solar production, thus the baseline control already results in a low energy bill and the potential for optimisation is low.

3.5. Influence of renovation scenario

This section compares how different renovation scenarios on the existing terraced house affect the performance of the GA algorithm controlling the operation of the PV system and the battery compared to the baseline control. Comparing the different scenarios (Fig. 10), it can be seen that for Strasbourg and Helsinki, the least favourable renovation scenarios lead to more absolute saving, while for the best renovation scenario it leads to more relative savings. For the non-deep retrofit cases (Cases 0 and 1), the relative savings are similar between the two locations with improvements of about 2.5% between the cases. There is a bigger increase when moving to deep retrofit scenarios (Cases 2 and 3), while the difference between the cases is smaller.

For Athens, the savings for the retrofit scenarios are almost null. Except for the case 0, the absolute saving would probably not be sufficient to justify a complex control system in the conditions presented in the paper.

3.6. Influence of the PV panel orientation

In this section, the influence of the PV panel orientation on the performance of the GA-based control algorithm is analysed. Regarding solar production, the most favourable orientation is south. With a south east orientation the production will be better in the morning while south west will have a better production in the afternoon. Then, it can be posited that the efficiency of a photovoltaic panel will be inversely proportional to the angle of inclination of the panel relative to the south.

Table 7
Yearly absolute savings achieve by the GA optimisation algorithm for different PV panel orientations.

Climate	Orientation Case	South	South West	West	East
Athens	Case 0	34.37	36.39	41.81	38.76
	Case 1 FC	18.40	19.82	23.02	21.11
	Case 1 Rad	13.18	13.95	16.25	15.41
	Case 2	1.56	1.42	2.01	1.76
	Case 3 FC	1.19	1.35	1.37	1.33
	Case 3 Rad	1.01	1.25	1.45	1.34
Helsinki	Case 0	225.58	227.79	232.13	231.90
	Case 1 FC	219.18	221.54	227.05	225.31
	Case 1 Rad	208.08	212.23	217.29	216.82
	Case 2	176.54	179.28	186.32	185.68
	Case 3 FC	168.29	171.55	179.92	178.30
	Case 3 Rad	160.44	163.26	172.50	170.08
Strasbourg	Case 0	148.42	148.91	154.24	158.12
	Case 1 FC	130.47	131.30	137.41	141.39
	Case 1 Rad	114.79	116.01	121.51	126.79
	Case 2	81.94	83.07	86.15	91.12
	Case 3 FC	70.16	70.54	74.32	78.24
	Case 3 Rad	60.16	60.11	63.89	67.49

Table 7 shows the absolute saving between the GA-based control and the rule-based baseline control for the terraced house cases for different PV panel orientations. It can be seen that the absolute savings are better for least favourable PV orientation. Whether this is East or West depends on whether there is more morning or afternoon sunlight.

In Helsinki, the savings from bigger to smaller go west, east, south west, and south. Because Strasbourg is more west of its time zone than Helsinki, meaning that there is more afternoon sun, the east yield more savings than west, as it is a less favourable case, thus having a bigger optimisation margin. This suggests that optimised control can compensate slightly for no-ideal PV installation, however the influence is limited compared to other factors investigated in this study. For example, the difference of relative savings linked to the PV panel orientation in Helsinki is less than 1% and only slightly above for the Strasbourg cases. The annual difference is only around 20 €.

Table 8
Strasbourg cases with different energy prices.

Case	Cost	Absolute Savings [€]	Relative Savings [%]
Case 0	France	148.91	15.57
	Greece	194.69	19.27
	Finland	161.24	22.75
Case 1 Rad	France	116.01	20.41
	Greece	153.57	25.35
	Finland	126.25	29.66
Case 3 Rad	France	60.11	25.33
	Greece	80.56	31.97
	Finland	65.77	36.54

In Athens, the pattern is less clear, because of the low saving potential of the optimisation algorithm. The South orientation leads to less saving in the different cases since it makes it more likely for the baseline scenario to be optimal.

3.7. Influence of the energy prices

Table 8 presents the influence of the different energy tariffs on the GA-based control performance on the Strasbourg cases. A similar pattern can be seen for the three cases considered. The Finnish energy costs incurs significantly higher relative saving than the French one, and the Greek energy costs provide bigger relative savings and absolute savings. This shows that the average energy cost is not the main driver to determine the cost savings of the control algorithm. It can be concluded that the intra-day signals are more important that the absolute energy cost to determine the final savings of the optimisation algorithm. Indeed, whether it is interesting to store energy in the battery at low energy cost, depends on the difference between low and high energy costs being bigger than the cost of the energy lost during the charge and discharge of the battery. Ultimately the price signals depend more on the energy mix of the country rather than the absolute cost of the energy.

4. Discussion

A GA-based control optimisation for a system with PV panels and electrical battery for a building with GSHP has been studies. The simple implementation due to the limited modelling that GA optimisation allows is a significant advantage in terms of applicability and repeatability. It has also been demonstrated that it can be easily transferred between use cases with similar system typologies, favouring the installation of GSHP and PV systems at a large scale.

The control algorithm performs a 24-hours horizon cost optimisation using predicted solar production and energy demand for the next 24-hours along with the current state of charge of the battery. In practice, only the first step of the optimised schedule is implemented and a new optimisation is performed every hour based on the updated forecasts and system conditions. This rolling-horizon approach enable to mitigate the fact that predictions uncertainties increase with time and counterbalances the tendency of the algorithm to deplete the battery over a 24-hour period.

Supposing that the retrofitting measures were already performed, thus not considering at the moment the related costs, the savings the optimised GA-based control strategy achieves compared to a more traditional rule-based control was evaluated in 87 different scenarios. The algorithm has shown to provide up to 202 € yearly savings for the terraced house typology and 474 € for the office block typology. However, the absolute cost is conservative because the energy costs used for the study do not take into account the taxes and the margin from the electrical companies. The actual absolute savings are likely to be bigger in practice. The relative savings can be up to 30% of the energy bill meaning less energy is imported from the grid and the locally produced solar energy is better exploited.

In general, in the different comparison performed, it was observed that if the energy demand is higher, the absolute savings are higher, while if the energy demand is smaller, the relative savings are bigger. This means that such algorithm can be an easy way to reduce the amount of energy taken form the grid and the amount of local solar production lost in case deep renovation cannot be afforded. In the case of deep renovation, it contributes to reducing the operational costs thus shortening the return on investment period. In light of the savings obtained, it cannot replace a careful design of the system, which will also impact on the return on investment.

The comparison of the scenarios shows that for buildings with high energy demand compared to the surface available for PV production, the absolute savings achieved by the algorithm can be significant although they might only achieve a small relative saving of the energy bill. Given that the installed photovoltaic surface area will be more closely aligned with the demand of a single-family residence, the relative impact will be more pronounced.

After the building typology, the climate play the biggest role on the saving achieved, not so much in relative saving, but in absolute saving. The GA-based control is more favourable in cold and mild climate as there is more potential to optimise the use of the battery. The orientation of the PV panel was found to have limited influence, while deeper renovation measures would lead to higher relative saving due to the reduced demand. The most significant factor influencing the outcome was the decision to renovate the building envelope.

One of the conditions for the algorithm to reduce costs by purchasing energy from the grid to charge the battery is that the difference between high and low prices is greater than the cost of energy loss during charging and discharging the battery. Indeed it was demonstrated that global energy prices were not directly proportional to the algorithm savings. This illustrates the impact of energy pricing and pricing policies can have on grid stability and flexibility. This also means that the long term benefit of such algorithm will be affected by changes in energy prices for example linked with geopolitics.

In certain scenarios, it was shown that the proposed optimisation did not result in sufficient savings to make the implementation of the GA-optimisation a worthwhile endeavour in comparison to the baseline algorithm. Indeed, on days where the solar production is particularly high, the optimisation reserve is correspondingly limited, as the energy demand can be fully covered by the PV production. The higher the frequency of these days, the lower the necessity of the optimisation algorithm. This is evident in the majority of the Athens cases proposed in this paper. The archetypes presented by [8] were designed to maximise the roof production based on the available roof space. This approach is logical for instances where solar radiation is limited, such as in Helsinki. In such cases, it is prudent to maximise the utilisation of PV panels to capture as much solar energy as possible. In the case of Athens, this only makes sense if selling excess energy to the grid is considered. Otherwise, it leads to oversizing, and it would be more economical to size according to the demand. The possibility of selling excess PV production to the grid allows the battery to contribute to electrical grid stability by storing energy at peak production and selling it at high demand times. However, this would require adaptations of the present algorithm. A cost–benefit analysis would be necessary to determine which of the two strategies is the most cost-effective and has a more positive impact on greenhouse gas emission reduction.

The sizing of the battery may also enable the system to be optimised and the control to be better taken advantage of. There are generally two main strategies when operating a battery: one is to use the battery until it is fully discharged, to optimise the charge period; the second is to not discharge beyond a certain threshold, which may damage the efficiency of the charging phase at some point. Which one is considered will affect the sizing of the battery. Given that Athens requires a significant amount of energy for cooling during the summer period, when there is also a high level of PV production, it is logical to size the battery according to the energy demand in order to achieve an optimal

charge/discharge. Conversely, in Helsinki, there is limited production both in summer and in winter, and there is also a more limited demand in summer. In order to implement an optimal strategy based on the market price without a high energy production, it is not advisable to oversize the battery, as this would be costly to maintain in winter. In this case, it is more prudent to size the battery based on the potential energy production linked to the installed PV capacity.

The fact that the benefit of the optimisation algorithm is affected by the installed PV capacity and the size of the battery suggests the importance to couple system sizing and control optimisation. The incorporation of this type of optimisation algorithm into the sizing process can facilitate a reduction in the size of the system, thereby making it more cost-effective.

The present study has been realised using energy demand based on a system with GSHP and PV. However, because the control algorithm has been designed to be high level, it could be implemented in cases either with different energy production sources (e.g. micro wind generation) or with other types of heat pumps. It would be necessary to re-reevaluate the actual savings because the changes in production and consumption patterns could affect the performance of the control strategy. As future work, it would be beneficial to conduct a similar study with a broader scope of the control algorithm, for example optimising the battery life using a multi-objective optimisation, including flexibility mechanism beyond price signal or adding the possibility to sell surplus solar energy to the grid to provide a flexible and transferable control algorithm that address the different problematic of this type of systems. For practical implementation, it would also be valuable to assess the impact of various uncertainties, including prediction errors in solar irradiance and load demand, and battery ageing, on the system economic performance. Finally, the influence of the sizing of the system on the savings would also be a relevant aspect to explore.

5. Conclusion

Starting from the hourly electricity demand of typical historic and existing urban buildings located in three European climates (warm, mild and cold), the replicability of an optimisation strategy based on a simple model of the energy system and a genetic algorithm optimisation have been studied on 87 scenarios. The studied buildings included a ground source heat pump, a photovoltaic system sized based on the space availability and considering different orientations, and a battery storage system. Additionally, several renovation strategies were considered for each case.

The optimisation is based on the assumption that the buildings' retrofit has already been completed. Furthermore, in a scenario where energy prices reflect the relation between the production and demand levels, the strategy involves storing energy in the battery when prices are low. This approach helps to reduce reliance on grid energy during peak times when prices are high and the grid is under stress.

The optimisation control algorithm proved to be cost-effective in mild and cold climates, with savings between 15% and 30% of savings on the energy bill compared to a reactive rule-based system. Although the results were less interesting for the warm climate cases, it is possible that adjustments to the system could lead to savings through the application of a similar optimisation algorithm. In general, in the cases with greater energy demand, optimisation led to bigger absolute saving, while reducing the energy demand led to greater relative savings. This phenomenon is observed in the case of existing buildings, where the starting conditions are more favourable compared to historical buildings. Furthermore, the same is true for increasing levels of building retrofitting. The potential impact of this type of algorithm on the energy grid, is likely to be greater if it is deployed on a larger scale, particularly in single-family buildings that are more suitable for the installation of a relatively high surface area of PV compared to the demand. In the case of larger buildings, although the absolute cost reduction is greater, the relative saving is only in the range of 2–3% for the cases considered.

It was also concluded that in order for the optimisation algorithm to effectively store energy in the battery when there is surplus energy in the grid (low energy prices), the intra-day price difference between low demand periods and the peak times when a reduction of consumption is desirable must be significant enough to offset the energy losses incurred during the charge and discharge cycles of the battery.

Considering the principal findings of this study, the optimal coupling of photovoltaic panel production and energy storage can effectively diminish grid dependency, thereby facilitating the transition towards a more efficient utilisation of renewable energy sources. Furthermore, the straightforward implementation resulting from the constrained modelling permitted by the GA optimisation represents a significant advantage in terms of applicability and repeatability.

CRediT authorship contribution statement

Sarah Noye: Writing – review & editing, Writing – original draft, Visualization, Validation, Software, Methodology, Investigation, Formal analysis, Data curation, Conceptualization. **Laura Carnieletto:** Writing – review & editing, Writing – original draft, Visualization, Validation, Software, Methodology, Investigation, Formal analysis, Data curation, Conceptualization. **Michele De Carli:** Writing – review & editing, Supervision, Project administration, Funding acquisition.

Declaration of competing interest

The authors declare that they have no known competing financial interests or personal relationships that could have appeared to influence the work reported in this paper.

Acknowledgements

This work was developed as part of the GEO4CIVHIC Project, which has received funding from the European Union's Horizon 2020 research and innovation program under grant agreement No. 792355.

Appendix. Detailed description of the model inputs

A.1. Climates

Simulations were carried out considering three different climates that were chosen to be representative of the main European climatic conditions, as already shown by [8,28]. Degree days have been used as parameter to group the archetypes according to the Köppen–Geiger scale [34,35]. Although the same country often presents more than one climate, four main groups have been defined based on the values of the heating and cooling degree days (HDD, CDD):

- Dry warm climates, including BWh (Hot desert climate) and BSk (Cold semi-arid climate)
- Mild warm climates, including Csa (Hot-summer Mediterranean climate), Csb (Warm-summer Mediterranean climate), Cfa (Humid subtropical climate)
- Mild cold climates, including Cfb (Temperate oceanic climate or subtropical highland climate) and Cfc (Subpolar oceanic climate)
- Cold climates, including Dfb (Humid continental climate) and Dfc (Subarctic climate)

However, the research focused on the use of GSHP for the refurbishment of buildings whose efficiencies are based on standardised profiles of energy (standard EN 14825 [36]). Therefore, the European climatic conditions have been grouped in 3 main cluster, identified by a reference city:

- Athens as representative of the warm climate, HDD = 995 and CDD = 1046;

Table A.9
Building envelope properties [8].

Type	Climate	U roof [W/(m^2 K)]	U walls [W/(m^2 K)]	U floor [W/(m^2 K)]	U windows [W/(m^2 K)]
Existing building	Athens	1.65	0.89	1.36	3.55
	Strasbourg	0.70	1.05	1.01	2.85
	Helsinki	0.29	0.35	0.41	2.35
Historic buildings	Athens	2.30	1.75	1.29	4.97
	Strasbourg	1.19	1.75	1.38	3.69
	Helsinki	0.54	1.11	0.79	2.72

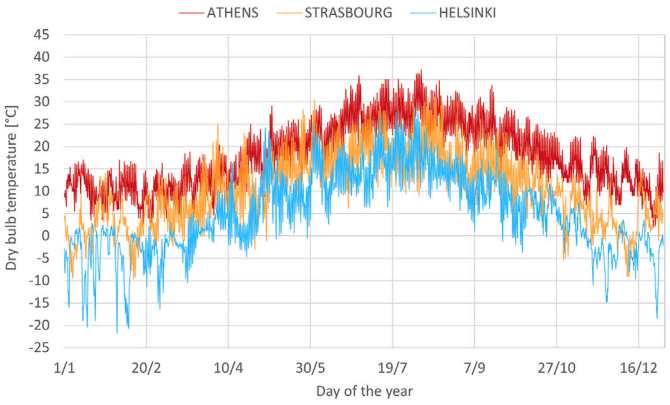

Fig. A.11. Hourly dry bulb temperature for the considered climates.

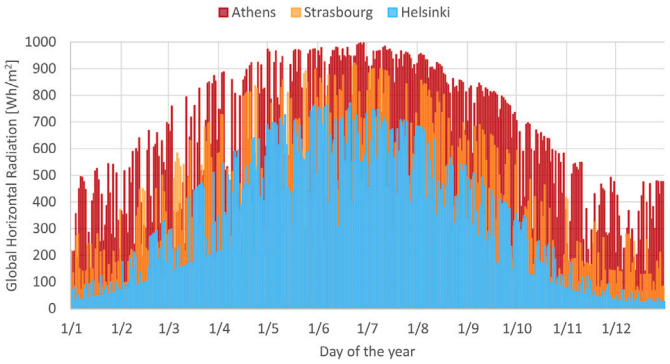

Fig. A.12. Hourly global horizontal radiation for the considered climates.

- Strasbourg for a mild climate, HDD = 2746 and CDD = 115;
- Helsinki as a cold climate, HDD = 4597 and CDD = 23.

where DDH and DDC have been calculated according to [37].

Fig. A.11 shows the hourly outdoor temperature of the considered locations, ranging from a maximum temperature of 37.2 °C in Athens, to 28.7 °C in Helsinki. Strasbourg as mild climate has a maximum temperature during the summer of about 31 °C, while the minimum is −9.7 °C compared to −21.7 °C of Helsinki and 2 °C of Athens.

Similarly, Fig. A.12 shows the significantly different solar radiation available at the three latitudes.

A.2. Building characteristics

The characteristics of the buildings used as input for the energy simulations have been presented in Table A.9. They have been considered based on the climates (Athens, Strasbourg and Helsinki) and studying the most common building construction techniques.

The terraced house has been studied considering a typical residential use, while the apartment block has been simulated both for residential and office use. Among the input data required for dynamic simulations, sensible loads related to typical residential use for a family of four people have been defined and scheduled based on Standard ISO 13790 [38]. EN 16798-1:2019 introduced reference values to set infiltration rates, assumed equal to 0.4 h^{-1} for non retrofitted buildings and 0.1 h^{-1} when envelope retrofit is simulated. These values were considered based on standards in order to have replicable and comparable results. The design lighting power generally corresponds to the sum of the power rating of each lamp installed in a room or area. Although subjective preferences and habits of the users may influence the standard values considered for lighting and electrical equipment, in this study typical reference values have been chosen according to standard EN 16798-1 [39]. Air set point temperature for space heating was set at 20 °C, considering as heating season the period between October and April and as daily schedule 7 a.m./9 p.m. If space cooling was needed during the summer, the temperature was set at 26 °C with a maximum relative humidity of 50%, from 10 a.m. to 12 p.m.

A.3. Geothermal system sizing

Ground source heat pumps (GSHP) are used to transfer heat to or from the ground due to the relatively constant temperature of the ground over the seasons. The GSHP performance is influenced by the thermal conductivity of the ground. Since the main goal of this work is to optimise the PV electric storage system, an average thermal conductivity of 2.2 W/(m K) and thermal capacity of 2.5 MJ/(m^3 K) have been considered from [8]. Results for more values have been presented in [8]. The required borehole lengths for heating (Lh) and cooling (Lc) was estimated implementing the ASHRAE method [40] with the excel tool developed by Capozza et al. [41]. The maximum possible length was set at 300 m according to the space availability for the urban context considered within a typical terraced house, while for the apartment block an upper limit of 1800 m was defined. The detailed sizing of GSHP systems was previously discussed in [8], where the probe configuration was designed to minimise thermal interference and prevent soil temperature imbalance.

Figs. A.13–A.15 show the comparison between the different heating systems in existing and historical buildings without (a) and with (b) retrofitted envelopes for each simulated climate. In Athens and Helsinki, the thermal load is unbalanced between the summer (Lc) and the winter season (Lh), as can be seen from the significant difference displayed in Fig. A.13a and A.15a. Since the penalty temperature calculated with the ASHRAE method was lower than 1 °C in all cases, ground thermal drift is excluded despite the unbalanced thermal load. The installation of envelope retrofit reduces transmission heat losses. As a consequence, the heating demand for space heating is greatly reduced for mild and cold climates, thus the required borehole length for heating and the electric energy required for the operation. The cooling length of the probe has a slight reduction, partially increasing the load unbalance only for warm climates (Athens). On the contrary, the significant reduction of Lh in mild (Strasbourg) and cold (Helsinki) climates contributes to the load balance. When load is unbalanced, specific criteria were defined to select the optimal length that satisfies energy requirements while avoiding subsidence and drift problems. Similar results were obtained for residential apartment blocks and office buildings. Therefore, envelope refurbishment contributes to a decrease of both probes' length and electric energy used by the heat pump, obtained by performance maps of real heat pumps.

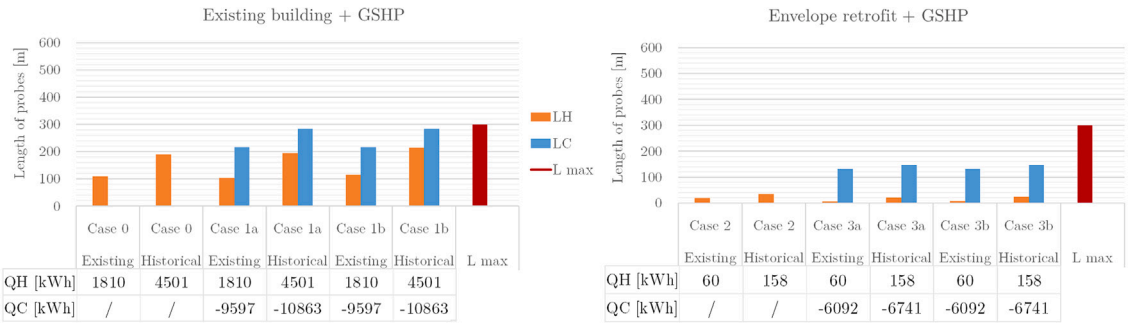

	Case 0 Existing	Case 0 Historical	Case 1a Existing	Case 1a Historical	Case 1b Existing	Case 1b Historical	L max
QH [kWh]	1810	4501	1810	4501	1810	4501	
QC [kWh]	/	/	-9597	-10863	-9597	-10863	

	Case 2 Existing	Case 2 Historical	Case 3a Existing	Case 3a Historical	Case 3b Existing	Case 3b Historical	L max
QH [kWh]	60	158	60	158	60	158	
QC [kWh]	/	/	-6092	-6741	-6092	-6741	

Fig. A.13. Borehole length comparison for Athens without (a) and with (b) envelope retrofit [8].

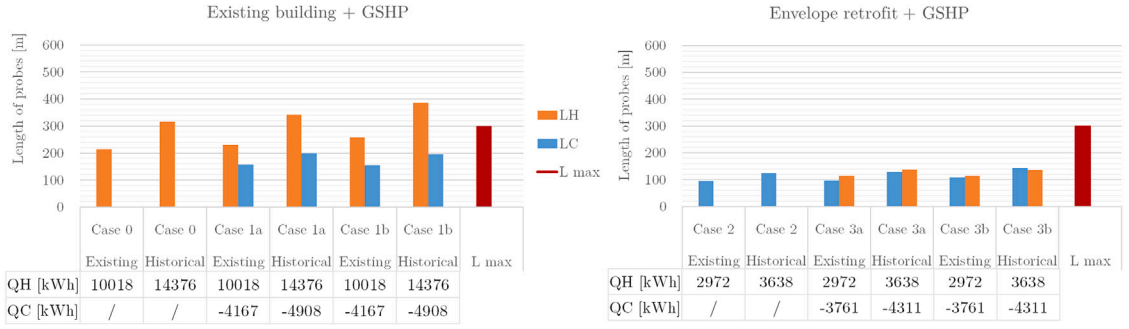

	Case 0 Existing	Case 0 Historical	Case 1a Existing	Case 1a Historical	Case 1b Existing	Case 1b Historical	L max
QH [kWh]	10018	14376	10018	14376	10018	14376	
QC [kWh]	/	/	-4167	-4908	-4167	-4908	

	Case 2 Existing	Case 2 Historical	Case 3a Existing	Case 3a Historical	Case 3b Existing	Case 3b Historical	L max
QH [kWh]	2972	3638	2972	3638	2972	3638	
QC [kWh]	/	/	-3761	-4311	-3761	-4311	

Fig. A.14. Borehole length comparison for Strasbourg without (a) and with (b) envelope retrofit [8].

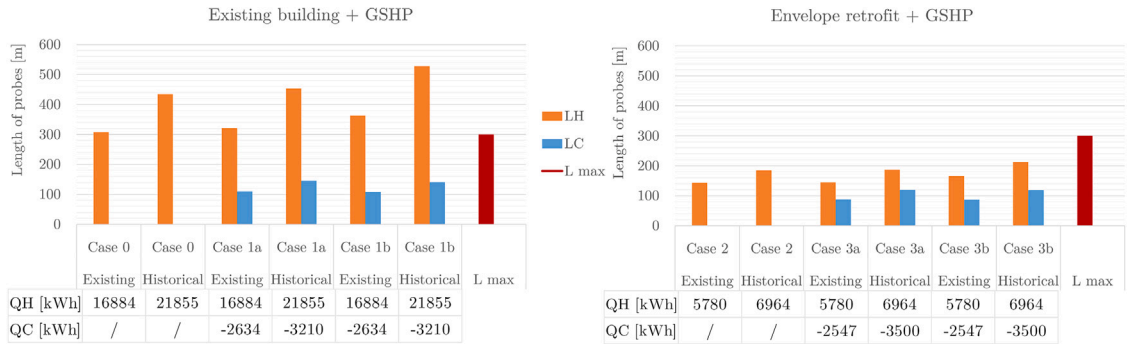

	Case 0 Existing	Case 0 Historical	Case 1a Existing	Case 1a Historical	Case 1b Existing	Case 1b Historical	L max
QH [kWh]	16884	21855	16884	21855	16884	21855	
QC [kWh]	/	/	-2634	-3210	-2634	-3210	

	Case 2 Existing	Case 2 Historical	Case 3a Existing	Case 3a Historical	Case 3b Existing	Case 3b Historical	L max
QH [kWh]	5780	6964	5780	6964	5780	6964	
QC [kWh]	/	/	-2547	-3500	-2547	-3500	

Fig. A.15. Borehole length comparison for Helsinki without (a) and with (b) envelope retrofit [8].

Data availability

Data will be made available on request.

References

[1] European Parliament and Council. Directive 2023/2413 on the promotion of the use of energy from renewable sources. 2023, Official Journal of the European Union.

[2] Maghrabie HM, Abdeltwab MM, Tawfik MHM. Ground-source heat pumps (GSHPs): Materials, models, applications, and sustainability. Energy Build 2023;299:113560. http://dx.doi.org/10.1016/j.enbuild.2023.113560.

[3] D'Agostino D, Minichiello F, Petito F, Renno C, Valentino A. Retrofit strategies to obtain a NZEB using low enthalpy geothermal energy systems. Energy 2022;239:122307. http://dx.doi.org/10.1016/j.energy.2021.122307.

[4] Poletto C, Dumont O, De Pascale A, Lemort V, Ottaviano S, Thomé O. Control strategy and performance of a small-size thermally integrated Carnot battery based on a Rankine cycle and combined with district heating. Energy Convers Manage 2024;302:118111. http://dx.doi.org/10.1016/j.enconman.2024.118111.

[5] Litjens G, Worrell E, van Sark W. Lowering greenhouse gas emissions in the built environment by combining ground source heat pumps, photovoltaics and battery storage. Energy Build 2018;180:51–71. http://dx.doi.org/10.1016/j.enbuild.2018.09.026.

[6] Poppi S, Sommerfeldt N, Bales C, Madani H, Lundqvist P. Techno-economic review of solar heat pump systems for residential heating applications. Renew Sustain Energy Rev 2018;81. http://dx.doi.org/10.1016/j.rser.2017.07.041.

[7] Pinamonti M, Prada A, Baggio P. Rule-based control strategy to increase photovoltaic self-consumption of a modulating heat pump using water storages and building mass activation. Energies 2020;13. http://dx.doi.org/10.3390/en13236282.

[8] Carnieletto L, Bella AD, Quaggiotto D, Emmi G, Bernardi A, De Carli M. Potential of GSHP coupled with PV systems for retrofitting urban areas in different European climates based on archetypes definition. Energy Built Environ 2024;5(3):374–92. http://dx.doi.org/10.1016/j.enbenv.2022.11.005.

[9] Noye S, Mulero Martinez R, Carnieletto L, De Carli M, Castelruiz Aguirre A. A review of advanced ground source heat pump control: Artificial intelligence for autonomous and adaptive control. Renew Sustain Energy Rev 2022;153:111685. http://dx.doi.org/10.1016/j.rser.2021.111685.

[10] Shabani M, Shabani M, Wallin F, Dahlquist E, Yan J. Smart and optimization-based operation scheduling strategies for maximizing battery profitability and longevity in grid-connected application. Energy Convers Manag: X 2024;21:100–519. http://dx.doi.org/10.1016/j.ecmx.2023.100519.

[11] Mathumitha R, Rathika P, Manimala K. Intelligent deep learning techniques for energy consumption forecasting in smart buildings: A review. Artif Intell Rev 2024;57(2):35. http://dx.doi.org/10.1007/s10462-023-10660-8.

[12] Baraskar S, Günther D, Wapler J, Lämmle M. Analysis of the performance and operation of a photovoltaic-battery heat pump system based on field measurement data. Sol Energy Adv 2024;4. http://dx.doi.org/10.1016/j.seja.2023.100047.

[13] Knuutinen J, Böök H, Ruuskanen V, Kosonen A, Immonen P, Ahola J. Ground source heat pump control methods for solar photovoltaic-assisted domestic hot water heating. Renew Energy 2021;177. http://dx.doi.org/10.1016/j.renene.2021.05.139.

[14] Chakir A, Tabaa M, Moutaouakkil F, Medromi H, Julien-Salame M, Dandache A, Alami K. Optimal energy management for a grid connected PV-battery system. Energy Rep 2020;6:218–31. http://dx.doi.org/10.1016/j.egyr.2019.10.040.

[15] Nottrott A, Kleissl J, Washom B. Energy dispatch schedule optimization and cost benefit analysis for grid-connected, photovoltaic-battery storage systems. Renew Energy 2013;55:230–40. http://dx.doi.org/10.1016/j.renene.2012.12.036.

[16] Ouedraogo KE, Ekim PO, Demirok E. Feasibility of low-cost energy management system using embedded optimization for PV and battery storage assisted residential buildings. Energy 2023;271:126922. http://dx.doi.org/10.1016/j.energy.2023.126922.

[17] Ranaweera I, Midtgård O-M. Optimization of operational cost for a grid-supporting PV system with battery storage. Renew Energy 2016;88:262–72. http://dx.doi.org/10.1016/j.renene.2015.11.044.

[18] Yang Y, Bremner S, Menictas C, Kay M. Modelling and optimal energy management for battery energy storage systems in renewable energy systems: A review. Renew Sustain Energy Rev 2022;167:112671. http://dx.doi.org/10.1016/j.rser.2022.112671.

[19] Liu Z, Mohammadzadeh A, Turabieh H, Mafarja M, Band SS, Mosavi A. A new online learned interval type-3 fuzzy control system for solar energy management systems. IEEE Access 2021;9:10498–508. http://dx.doi.org/10.1109/ACCESS.2021.3049301.

[20] Judge MA, Franzitta V, Curto D, Guercio A, Cirrincione G, Khattak HA. A comprehensive review of artificial intelligence approaches for smart grid integration and optimization. Energy Convers Manag: X 2024;24:100–724. http://dx.doi.org/10.1016/j.ecmx.2024.100724.

[21] Molu RJJ, Raoul Dzonde Naoussi S, Wira P, Mbasso WF, Kenfack ST, Kamel S. Optimization-based energy management system for grid-connected photovoltaic/battery microgrids under uncertainty. Case Stud Chem Environ Eng 2023;8:100464. http://dx.doi.org/10.1016/j.cscee.2023.100464.

[22] Hossain Lipu MS, Ansari S, Miah MS, Hasan K, Meraj ST, Faisal M, Jamal T, Ali SHM, Hussain A, Muttaqi KM, Hannan MA. A review of controllers and optimizations based scheduling operation for battery energy storage system towards decarbonization in microgrid: Challenges and future directions. J Clean Prod 2022;360:132188. http://dx.doi.org/10.1016/j.jclepro.2022.132188.

[23] Katoch S, Chauhan SS, Kumar V. A review on genetic algorithm: Past, present, and future. Multimedia Tools Appl 2021;80(5):8091–126. http://dx.doi.org/10.1007/s11042-020-10139-6, arXiv:33162782.

[24] Teng J-H, Luan S-W, Lee D-J, Huang Y-Q. Optimal charging/discharging scheduling of battery storage systems for distribution systems interconnected with sizeable PV generation systems. IEEE Trans Power Syst 2013;28(2):1425–33. http://dx.doi.org/10.1109/TPWRS.2012.2230276.

[25] Lujano-Rojas JM, Dufo-López R, Bernal-Agustín JL, Catalão JPS. Optimizing daily operation of battery energy storage systems under real-time pricing schemes. In: 2017 IEEE manchester powerTech. 2017, http://dx.doi.org/10.1109/PTC.2017.7981255.

[26] De Carli M, Carnieletto L, Di Bella A, Graci S, Emmi G, Zarrella A, Baseggio N, Belliardi M, Rossi L, Mulè Stagno L, et al. Archetype definition for analysing retrofit solutions in urban areas in europe. In: 13th REHVA world congress CLIMA, vol. 111, 2019, http://dx.doi.org/10.1051/e3sconf/201911103027.

[27] TRNSYS 17 - a TRaNsient system simulation program. 2014, Reference manual, Solar Energy Laboratory, Univ. of Wisconsin-Madison.

[28] Carnieletto L, Badenes B, Belliardi M, Bernardi A, Graci S, Emmi G, Urchueguía J, Zarrella A, Di Bella A, Dalla Santa G, Galgaro A, Mezzasalma G, De Carli M. A European database of building energy profiles to support the design of ground SourceHeat pumps. Energies 2019;12(13). http://dx.doi.org/10.3390/en12132496.

[29] Institut Wohnen und Umwelt. The joint EPISCOPE and TABULA website. 2016, https://episcope.eu.

[30] Hesaraki A, Huda N. A comparative review on the application of radiant low-temperature heating and high-temperature cooling for energy, thermal comfort, indoor air quality, design and control. Sustain Energy Technol Assessments 2022;49:101661. http://dx.doi.org/10.1016/j.seta.2021.101661.

[31] Wilson E, Metzger C, Horowitz S, Hendron R. NREL/TP-5500-60988: building america house simulation protocols. Tech. rep., National Renewable Energy Laboratory; 2014.

[32] Ollas P, Thiringer T, Persson M, Markusson C. Energy loss savings using direct current distribution in a residential building with solar photovoltaic and battery storage. Energies 2023;16(33):1131. http://dx.doi.org/10.3390/en16031131.

[33] Pandey HM, Chaudhary A, Mehrotra D. A comparative review of approaches to prevent premature convergence in GA. Appl Soft Comput 2014;24:1047–77. http://dx.doi.org/10.1016/j.asoc.2014.08.025.

[34] European Parliament and Council. Directive 2002/91/CE on the energy performances of buildings, L1/65. 2003, Official Journal of the European Union.

[35] European Parliament and Council. Directive 2010/31/EU on the energy performances of buildings (recast). 2010, Official Journal of the European Union.

[36] Air conditioners, liquid chilling packages and heat pumps, with electrically driven compressors, for space heating and cooling - testing and rating at part load conditions and calculation of seasonal performance. European standard EN 14825:2022, CEN/TC 113/WG 7: Heat Pumps, air conditioners and chilling liquid packages - testing and rating at part load conditions; 2022.

[37] De Carli M, Bernardi A, Cultrera M, Dalla Santa G, Di Bella A, Emmi G, Galgaro A, Graci S, Mendrinos D, Mezzasalma G, Pasquali R, Pera S, Perego R, Zarrella A. A database for climatic conditions around europe for promoting GSHP solutions. Geosciences 2018;8(71). http://dx.doi.org/10.3390/geosciences8020071.

[38] Energy performance of buildings – Calculation of energy use for space heating and cooling. ISO standard EN ISO 13790, Geneva, Switzerland; 2008.

[39] Energy performance of buildings - Ventilation for buildings - Part 1: Indoor environmental input parameters for design and assessment of energy performance of buildings addressing indoor air quality, thermal environment, lighting and acoustics. ISO Standard EN 16798:2019, Brussels, Belgium; 2019.

[40] ASHRAE American Society of Heating Refrigerating and Air-Conditioning Engineers. Ashrae handbook — hvac applications. Geothermal energy. Atlanta, GA; 2011.

[41] Capozza A, Zarrella A, Carli MD. Long-term analysis of two GSHP systems using validated numerical models and proposals to optimize the operating parameters. Energy Build 2015;93:50–64. http://dx.doi.org/10.1016/j.enbuild.2015.02.005.